

# A solar dynamo in the overshoot layer: cycle period and butterfly diagram

G. Rüdiger<sup>1,2</sup> and A. Brandenburg<sup>2</sup>

<sup>1</sup> Astrophysikalisches Institut Potsdam, An der Sternwarte 16, D-14482 Potsdam, Germany

<sup>2</sup> HAO/NCAR\*, P.O. Box 8000, Boulder, CO 80307, USA

Received 21 April 1994 / Accepted 17 September 1994

**Abstract.** We construct a solar dynamo model for the overshoot layer where a strong gradient in the turbulence velocity is assumed to produce the  $\alpha$ -effect. A recent rotation law from helioseismology is adopted and meridional flows are ignored. Since in the overshoot layer the convective turnover time is long compared with the rotation period, the full structure of the alpha and turbulent diffusion tensors appearing in the expressions for the turbulent electromotive force (EMF) must be retained in the computations. The important toroidal component of  $\alpha$  is *negative* in the overshoot layer. In this layer the turbulence is considered as rarefied with a “dilution factor”  $\epsilon < 1$  to account for the reduced EMF due to the intermittent nature of the magnetism. The cycle period increases with decreasing  $\epsilon$ , and for  $\epsilon \approx 0.2 - 0.5$  the 22 yr solar cycle period is reproduced, depending on details of the model. The effect of magnetic buoyancy can increase the cycle period further. If this layer is thinner than  $\approx 30$  Mm, the number of toroidal field belts is too large compared to the sun. Due to the strong rotational influence on the turbulence in the presence of a sharp change of the turbulence intensity at the bottom of the convection zone, the  $\alpha$ -effect is more concentrated to the equatorial region. This leads to more realistic butterfly diagrams. Observations indicate, however, that radial and azimuthal field components are out of phase, which is not reproduced by our model.

**Key words:** magnetohydrodynamics – turbulence – Sun: magnetic fields – stars: magnetic fields

---

## 1. Introduction

There are a considerable number of recent reviews on the solar dynamo, indicating the great interest in this topic. Nevertheless, there is no satisfactory model that reproduces the observed

*Send offprint requests to:* G. Rüdiger

\* The National Center for Atmospheric Research is sponsored by the National Science Foundation

magnetic field geometry and that is compatible with helioseismology and turbulence theory.

Over the past decade a number of theoretical arguments have lead to the consensus that the solar dynamo operates in the overshoot layer between the convection zone proper and the radiative interior; for recent reviews see Gilman (1992) and Schmitt (1993). This picture is motivated by the suggestion that the magnetic field is organized in the form of strong magnetic flux tubes whose motions are strongly controlled by magnetic buoyancy. In the convection zone the typical rise time of magnetic flux tubes is short, and only in the overshoot layer can magnetic flux tubes be stored over time scales comparable with the solar cycle period (Moreno-Insertis 1983). Furthermore, in order to understand the systematic orientation of magnetic bipolar regions at the solar surface, the Parker-Babcock picture of a toroidal magnetic flux tube breaking through the surface is often invoked. It is expected that such flux tubes will originate from deep layers (Parker 1975) and they must then be strong enough to resist significant distortion by the convective motions and the Coriolis force during their rise through the convection zone (Schüssler 1983, 1987; D’Silva 1993).

While there are convincing arguments that there is a strong systematic mean magnetic field at the bottom of the convection one, it still remains questionable whether this field is also generated there (Parker 1993). Instead, it might be generated in the entire convection zone, but continuously pumped into the overshoot layer by the convective motions where it accumulates (Nordlund et al. 1992). This latter suggestion is supported by the fact that the generation of magnetic fields in the overshoot layer alone faces severe problems. Firstly, this layer is so thin that in order to generate the magnetic flux observed at the surface, the magnetic field strength in this layer must exceed the equipartition value (Durney et al. 1990). Secondly, if the mean magnetic field is generated by an  $\alpha$ -effect in the overshoot layer, a rather sharp change of the turbulence intensity is required, which may be unrealistic. Thirdly, in a thinner layer the turbulent magnetic diffusion time is shorter and it is therefore more difficult to produce magnetic cycle periods as long as the 22 year cycle period of the sun.

Mixing length models of the solar convection zone, on the other hand, do indeed predict a sudden jump in the turbulent velocity that is needed to produce an  $\alpha$ -effect in the overshoot layer. Although mixing length models are not very accurate here, we now consider the possibility that the  $\alpha$ -effect generated in this layer is sufficiently strong. We allow for the possibility that the effective electromotive force is reduced in this layer, which decreases not only the  $\alpha$ -effect but especially the turbulent diffusivity. Furthermore, the turnover time is long and rotational effects on the turbulence are important. This leads to highly anisotropic  $\alpha$  and turbulent diffusivity tensors, and we use the corresponding expressions in the numerical solutions of the dynamo equations.

## 2. The turbulence effects

The evolution of the mean magnetic field  $\bar{\mathbf{B}}$  is governed by the dynamo equation

$$\frac{\partial \bar{\mathbf{B}}}{\partial t} = \text{rot}(\bar{\mathbf{u}} \times \bar{\mathbf{B}} + \mathcal{E}), \quad (1)$$

where  $\mathcal{E}$  is the turbulent electromotive force and  $\bar{\mathbf{u}}$  the mean velocity (Krause & Rädler 1980). We employ both spherical polar coordinates,  $(r, \theta, \varphi)$ , and cylindrical polar coordinates,  $(\varpi, \varphi, z)$ , where  $\varpi = r \sin \theta$  and  $z = r \cos \theta$ , assuming axisymmetry,  $\partial/\partial\varphi = 0$ . Helioseismology now provides detailed information about the profile of the internal angular velocity of the sun,  $\Omega = \bar{u}_\varphi/(r \sin \theta)$ . It is therefore reasonable to assume the differential rotation to be given and to focus attention on the induction effects arising from  $\mathcal{E}$ . As usual, we assume approximate scale separation and write

$$\mathcal{E}_i = \alpha_{ij} \bar{B}_j + \eta_{ijk} \bar{B}_{j,k} + \dots \quad (2)$$

The convergence of this approximation becomes especially questionable in the overshoot layer where the correlation length is likely to be comparable with the typical scale over which  $\bar{\mathbf{B}}$  varies. Keeping in mind that in an overshoot dynamo higher derivative terms might also be important, we now apply such a model to the sun and ask the question whether the solar magnetic field can be explained by such a model.

Almost all models presented hitherto assume the simplification

$$\alpha_{ij} = \alpha \delta_{ij}, \quad \eta_{ijk} = \eta_T \epsilon_{ijk}. \quad (3)$$

This formulation would only be correct if the turbulence was isotropic and helical. In a star helicity is generated by the combined action of rotation and stratification (Krause & Rädler 1980). Therefore the  $\alpha$ -tensor only exists if there is both rotation and stratification (i.e. inhomogeneity) of density and/or turbulence intensity. Furthermore, the  $\alpha$ -tensor is anisotropic, even in the case of slow rotation where the correlation time  $\tau_{\text{corr}}$  is short compared with the rotation period  $T_{\text{rot}}$ . It is convenient to express the tensorial structure in terms of the unit vector  $\hat{\mathbf{z}} = \Omega/\Omega$ , where  $\Omega$  is the basic rotation, whose magnitude is

measured in terms of the Coriolis number (proportional to the inverse Rossby number)

$$\Omega^* = 2 \tau_{\text{corr}} \Omega. \quad (4)$$

Stratification provides a further preferred direction to the turbulence. For the overshoot layer the stratification in the turbulence intensity is most important, because of the presumed sudden change of the turbulence velocity with depth. This is described by the vector  $\mathbf{U} = \nabla \eta_0$ , where

$$\eta_0 = \frac{1}{3} \epsilon \tau_{\text{corr}} \langle \mathbf{u}^2 \rangle \quad (5)$$

is a reference value for the turbulent magnetic diffusivity for slow rotation. Here we have introduced a ‘‘dilution factor’’  $\epsilon$ , which is usually taken as unity, the value obtained in the quasi-linear (first-order-smoothing) approximation. In the sun we expect  $\epsilon < 1$ , because of the reduced interaction between the turbulence and the magnetic fields caused by the intermittent nature of velocity and magnetic fields. We regard the turbulence in the overshoot layer as being controlled by a small number of intense plume-like events, where  $\epsilon$  measures the efficiency of the turbulent EMF. With three-dimensional turbulence simulations it should in principle be possible to obtain an estimate for this quantity, but in the following we consider  $\epsilon$  as a free parameter that may be adjusted in order to match the observations.

### 2.1. The $\alpha$ -tensor

Restricting ourselves to terms linear in  $\mathbf{U}$ , but allowing for arbitrary values of  $\Omega^*$ , we have

$$\begin{aligned} \alpha_{ij} = & \frac{3}{4} \Omega^* [-\psi(\hat{z}_k U_k) \delta_{ij} + \psi_\varpi(\hat{z}_i U_j + \hat{z}_j U_i)] c_\alpha \\ & + \frac{3}{4} \Omega^* [(2\psi_z + \psi - 2\psi_\varpi)(\hat{z}_k U_k) \hat{z}_i \hat{z}_j] c_\alpha \\ & - \epsilon_{ikl} U_k [\phi_1 \delta_{jl} + (\phi_2 - \phi_1) \hat{z}_j \hat{z}_l], \end{aligned} \quad (6)$$

where  $\Omega^* = \Omega^*(r, \theta)$ . (The limitation resulting from only keeping terms linear in  $\mathbf{U}$  is discussed in §2.3.) In Eq. (6), the  $\psi$ -terms are multiplied by a factor  $c_\alpha \leq 1$ , which can be adjusted to obtain a marginally excited dynamo. The  $\phi$ -terms represent the turbulent diamagnetism of an inhomogeneous turbulence field, and the  $\psi$ -terms form the symmetric part of the  $\alpha$ -tensor. In our formulation, the coefficient functions are even in the rotation rate. The evaluation of the coefficients  $\psi$  and  $\phi$  in closed form is only possible for certain simple turbulence models. For a turbulence model based on the mixing length formulation, Rüdiger & Kitchatinov (1993) found, for arbitrary rotation rates,

$$\psi = \frac{1}{\Omega^{*4}} \left( 9 + \Omega^{*2} - \frac{9 + 4\Omega^{*2} - \Omega^{*4}}{\Omega^*} \arctan \Omega^* \right), \quad (7)$$

$$\psi_z = \frac{1}{\Omega^{*4}} \left( \frac{9 + 7\Omega^{*2}}{1 + \Omega^{*2}} - \frac{\Omega^{*2} + 9}{\Omega^*} \arctan \Omega^* \right), \quad (8)$$

$$\psi_\varpi = \frac{3}{\Omega^{*4}} \left( -3 + \frac{\Omega^{*2} + 3}{\Omega^*} \arctan \Omega^* \right), \quad (9)$$

$$\phi_1 = \frac{3}{4\Omega^{*2}} \left( -1 + \frac{\Omega^{*2} + 1}{\Omega^*} \arctan \Omega^* \right), \quad (10)$$

$$\phi_2 = \frac{3}{2\Omega^{*2}} \left( 1 - \frac{\arctan \Omega^*}{\Omega^*} \right). \quad (11)$$

(Note that  $\phi_1 - \phi_2 = \frac{1}{4}\Omega^{*2}\psi_\varpi \geq 0$ .) Clearly, the  $\alpha$ -tensor is not at all isotropic. In cylindrical polar coordinates  $(\varpi, \varphi, z)$  we get

$$\alpha = \frac{d\eta_0}{dr}$$

$$\begin{pmatrix} -\frac{3}{4}c_\alpha\Omega^*\psi \cos \theta & \phi_1 \cos \theta & \frac{3}{4}c_\alpha\Omega^*\psi_\varpi \sin \theta \\ -\phi_1 \cos \theta & -\frac{3}{4}c_\alpha\Omega^*\psi \cos \theta & \phi_2 \sin \theta \\ \frac{3}{4}c_\alpha\Omega^*\psi_\varpi \sin \theta & -\phi_1 \sin \theta & \frac{3}{2}c_\alpha\Omega^*\psi_z \cos \theta \end{pmatrix}. \quad (12)$$

The case of *rapid* rotation,  $\Omega^* \gg 1$ , may be illustrated by retaining only terms of the order  $\Omega^{*-1}$  and larger, which leads to

$$\alpha = \begin{pmatrix} -\frac{3\pi}{8}c_\alpha \cos \theta & \frac{3\pi}{8\Omega^*} \cos \theta & 0 \\ -\frac{3\pi}{8\Omega^*} \cos \theta & -\frac{3\pi}{8}c_\alpha \cos \theta & 0 \\ 0 & -\frac{3\pi}{8\Omega^*} \sin \theta & 0 \end{pmatrix} \frac{d\eta_0}{dr}. \quad (13)$$

The  $\alpha_{zz}$ -component approaches zero most rapidly with  $\Omega^*$ . Furthermore,  $\alpha_{ij}\hat{B}_j$  no longer depends on the vertical component of the magnetic field. Note that for all values of  $\Omega^*$  the interesting relation

$$\left| \frac{u_{\text{dia}}}{\alpha} \right| \simeq \left| \frac{\alpha_{\varpi\varphi}}{\alpha_{\varphi\varphi}} \right| \simeq \frac{1}{\Omega^*} \quad (14)$$

holds, where  $u_{\text{dia}}$  represents the components of  $\alpha$  that are proportional to  $\phi_1$ . For sufficiently slow rotation the dynamo must thus turn off as the turbulent diamagnetic effect,  $u_{\text{dia}}$ , becomes so strong that the magnetic field is advected away faster than it can be regenerated by the  $\alpha$ -effect. (This is an important feature of dynamos with a localized  $\alpha$ .) For the overshoot dynamos investigated below we find that for  $d/R = 0.05$  and  $\epsilon = 1$  the critical Coriolis number for dynamo action is  $\Omega^* \approx 1.5$  (i.e.  $\tau_{\text{corr}}/T_{\text{rot}} \approx 0.12$ ). This number is not small, and the assumption of slow rotation, that has sometimes been made implicitly by ignoring anisotropies of  $\alpha$  and  $\eta$ , is *not valid*. Moreover, stars with  $\Omega^* < 1.5$  are expected to show no large scale magnetic fields (but they may still be active due to small scale dynamo action, see Durney et al. 1993). For the sun,  $\Omega^* \approx 5$ , and so we have to use the full equations (7)-(11).

## 2.2. The turbulent magnetic diffusivity tensor

We now turn to the turbulent magnetic diffusivity tensor. It exists even in the absence of a basic rotation. When there are no anisotropies it is simply  $\eta_{ijk} = \eta_T \epsilon_{ijk}$ . In the presence of rotation, the eddy diffusivity is decreased and  $\eta_{ijk}$  becomes anisotropic:

$$\eta_{ijk} = \eta_T \epsilon_{ijk} + (\eta_{\parallel} - \eta_T) \epsilon_{ijl} \hat{z}_l \hat{z}_k, \quad (15)$$

with

$$\eta_T = (\phi_1 + \phi_2)\eta_0, \quad \eta_{\parallel} = 2\phi_1\eta_0 \quad (16)$$

(Kitchatinov et al. 1994), where  $\phi_1$  and  $\phi_2$  were given in (10) and (11). The expressions  $\psi, \psi_z, \psi_\varpi, \phi_1$ , and  $\phi_2$  completely describe the influence of the basic rotation on the turbulent EMF. They all are derived from the same turbulence model.

Note that, since  $\phi_1 - \phi_2 \geq 0$ , the diffusivity is enhanced in the direction of  $z$ , as can be seen by taking the rot of the diffusion term:

$$\text{rot } \mathcal{E} = \dots + \left[ \eta_T \left( \frac{\partial^2}{\partial x^2} + \frac{\partial^2}{\partial y^2} \right) + \eta_{\parallel} \frac{\partial^2}{\partial z^2} \right] \bar{\mathbf{B}}. \quad (17)$$

This expression is only valid in Cartesian geometry and for constant  $\eta_T$  and  $\eta_{\parallel}$ . Using some vector algebra the diffusive contribution to the EMF can be rewritten in the form

$$\mathcal{E} = \dots - \eta_{\parallel} \mu_0 \bar{\mathbf{J}} + (\eta_{\parallel} - \eta_T) (\hat{\mathbf{z}} \mu_0 \bar{J}_z - \hat{\mathbf{z}} \times \nabla \bar{B}_z), \quad (18)$$

where  $\bar{\mathbf{J}} = \text{rot } \bar{\mathbf{B}}/\mu_0$  is the mean electrical current and  $\mu_0$  the vacuum permeability. In (18), which is now valid for nonuniform  $\eta_T$  and  $\eta_{\parallel}$ , only standard rot and grad operators are used, which are easy to implement in arbitrary geometry. In this formulation the magnetic diffusion in the direction away from the rotation axis is subtracted (second term in brackets), which is advantageous for an implicit (or semi-implicit) treatment of the isotropic diffusion term. Note also that the term  $-\phi_1 \mathbf{U} \times \bar{\mathbf{B}}$  in Eq. (6), corresponding to turbulent diamagnetism, can be written as  $-\frac{1}{2} \nabla \eta_{\parallel} \times \bar{\mathbf{B}}$ . An expression of this form has been obtained by Vainshtein & Zeldovich (1972) for the isotropic case.

## 2.3. Higher order terms in $\mathbf{U}$

There is a fundamental shortcoming in that the expressions above are only complete to first order in  $\mathbf{U}$ , the immediate consequence being that factors such as  $\Omega \cdot \mathbf{U} \propto \cos \theta$  appear linearly in the expressions for  $\alpha$ . The diagonal components, for example, are therefore proportional to  $\cos \theta$ , whereas higher order terms, including those proportional to  $\cos^3 \theta$ , are always ignored. Thus, the expressions for  $\alpha$  are certainly incorrect at high latitudes. Unfortunately, the coefficients for higher order terms in  $\Omega \cdot \mathbf{U}$  cannot be solved in closed form. The hope is that numerical simulations will soon be able to provide better estimates for the latitudinal dependence of  $\alpha$ . In the present paper we allow for an additional factor  $[1 - \alpha_U (\hat{\mathbf{z}} \cdot \mathbf{U})^2]$  multiplying the  $\psi$ -terms in Eq. (6), and consider  $\alpha_U$  to be a free parameter. It turns out that this parameter plays an important role for determining the latitudinal dependence of the magnetic field. For  $\alpha_U = 0$  the  $\alpha$ -effect is maximal at the poles and, together with the presumably strong radial gradients in the solar rotation law at high latitudes, this can cause intense magnetic fields at the poles. This is in contrast to the solar butterfly diagram showing that most of the sunspot activity occurs at low latitudes.

In order to study the influence of a reduced  $\alpha$ -effect at high latitudes we consider in the following two cases:  $\alpha_U = 0$  (i) and  $\alpha_U = 1$  (ii). In case (i) the  $\alpha$ -effect has a maximum at the poles,

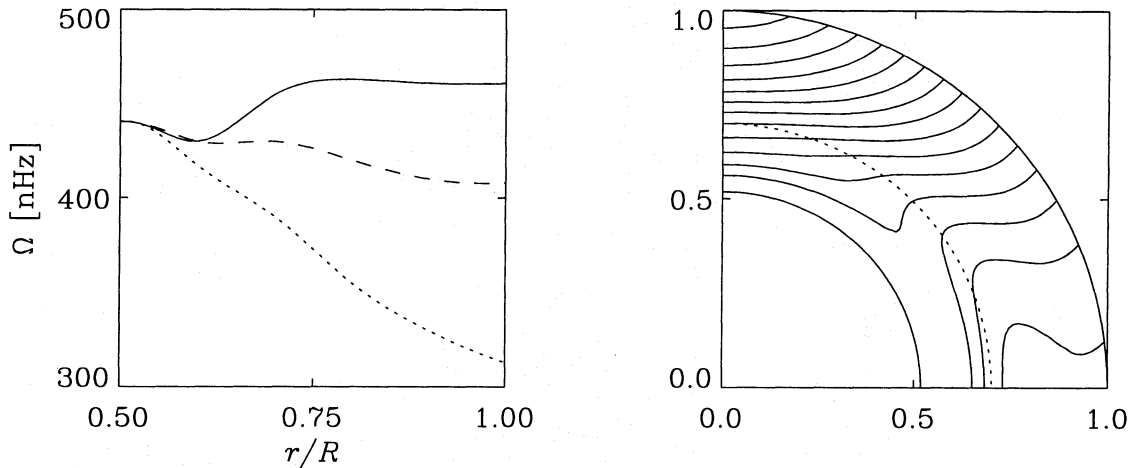


**Fig. 1.** Differential rotation law assumed in the computations. The radial profiles of  $\Omega$  (in nHz), adopted from the inversion of Christensen-Dalsgaard & Schou (1988). The left panel shows the radial dependence of the angular velocity at the equator (solid line), at  $45^\circ$  (dashed), and at the pole (dotted). The right panel shows contours of angular velocity in the meridional plane

while in (ii) it vanishes there and has a maximum at  $35^\circ$ . Apart from the possibility of negative polar values ( $\alpha_U > 1$ ), these provide two representative cases. An  $\alpha$ -effect concentrated at low latitudes has occasionally been considered (Yoshimura 1975; Schmitt 1987; Tuominen et al. 1988; Belvedere et al. 1991; Prautzsch 1993). In all those papers isotropic  $\alpha$ - and  $\eta$ -tensors were assumed, however.

#### 2.4. Nonlinear models

As the mean magnetic field approaches the equipartition value, the components of the  $\alpha$ - and  $\eta$ -tensors become affected non-uniformly. Unfortunately, these quenching expressions are so far only known for slow rotation (Rüdiger & Kitchatinov 1993). Therefore we study simple nonlinear ( $\alpha$ -quenched) solutions by replacing  $c_\alpha$  by  $1/(1 + \beta^2)$ , where  $\beta = |\bar{\mathbf{B}}|/B_{\text{eq}}$ . Here,  $B_{\text{eq}}(r)$  is the equipartition magnetic field strength with  $B_{\text{eq}}^2 = \mu_0 \rho u_t^2$ , and  $u_t = \langle u^2 \rangle^{1/2}$  is the rms-velocity of the turbulence. Vainshtein & Cattaneo (1992) argue that the quenching of  $\alpha$  should actually be much stronger. However, this remains debatable and Brandenburg et al. (1993) have presented evidence for only mild quenching, but a somewhat reduced kinematic value of  $\alpha$ , suggesting that  $c_\alpha < 1$ . Thus, it is plausible that in our model the field strengths quoted below are by an order of magnitude too large.

In some cases we also present models where the effects of turbulent and mean-field buoyancy have been included (Kitchatinov & Rüdiger 1992; Kitchatinov & Pipin 1993), by adding a term  $\mathbf{U}_{\text{buoy}} \times \bar{\mathbf{B}}$  on the right hand side of Eq. (2), where

$$\mathbf{U}_{\text{buoy}} = c_{\text{buoy}} \epsilon u_t \mathcal{H}_{\text{buoy}}(\beta) \hat{\mathbf{r}} \quad (19)$$

and

$$\mathcal{H}_{\text{buoy}} = \frac{1}{8\beta^2} \left( -\frac{3 + 5\beta^2}{(1 + \beta^2)^2} + \frac{3}{\beta} \arctan \beta \right). \quad (20)$$

The  $\Omega^*$  dependence of this expression is unknown. We therefore introduced the factor  $c_{\text{buoy}}$  in Eq. (19). (For  $c_{\text{buoy}} = 1$  the dynamo is no longer oscillatory, and so we take  $c_{\text{buoy}} = 0.5$  in all cases below.)

#### 2.5. The quasilinear approximation

The expressions concerning the turbulent EMF have been computed in the quasilinear approximation – also known as the second-order correlation approximation (SOCA). This approach is justified for short-correlated turbulence with small Strouhal number  $S = u_t \tau_{\text{corr}} / \ell$ . For stellar convection as well as for interstellar turbulence, however,  $S$  is of the order of unity. For the particular case of isotropic turbulence, Carvalho (1992) constructed an  $\alpha$ -effect as well as an eddy diffusivity for arbitrary values of the Strouhal number. For large values of  $S$  the  $\alpha$ -effect is strongly reduced, but for the solar case of  $S \simeq 1$  the reduction is by no more than 30%.

Meanwhile there is another important argument that may justify the application of the SOCA even for  $S \simeq 1$ . Interstellar turbulence driven by supernova explosions has been investigated both analytically (Ferrière 1993) as well as numerically (Kaisig et al. 1993; Ziegler et al. 1994). The latter, however, does not rely on the SOCA, and yet the results are qualitatively very similar (see, e.g., the negativity of the  $\alpha_{zz}$  component), and the quantitative agreement may be considered as an independent proof for the validity of the results obtained with SOCA.

However, for the case of rapid rotation which is necessary to match the stellar situation there are at the moment no possibilities to discuss the SOCA results in comparison to more exact procedures.

### 3. The overshoot dynamo

Following the arguments given in the introduction we place the dynamo in the overshoot layer between the convection

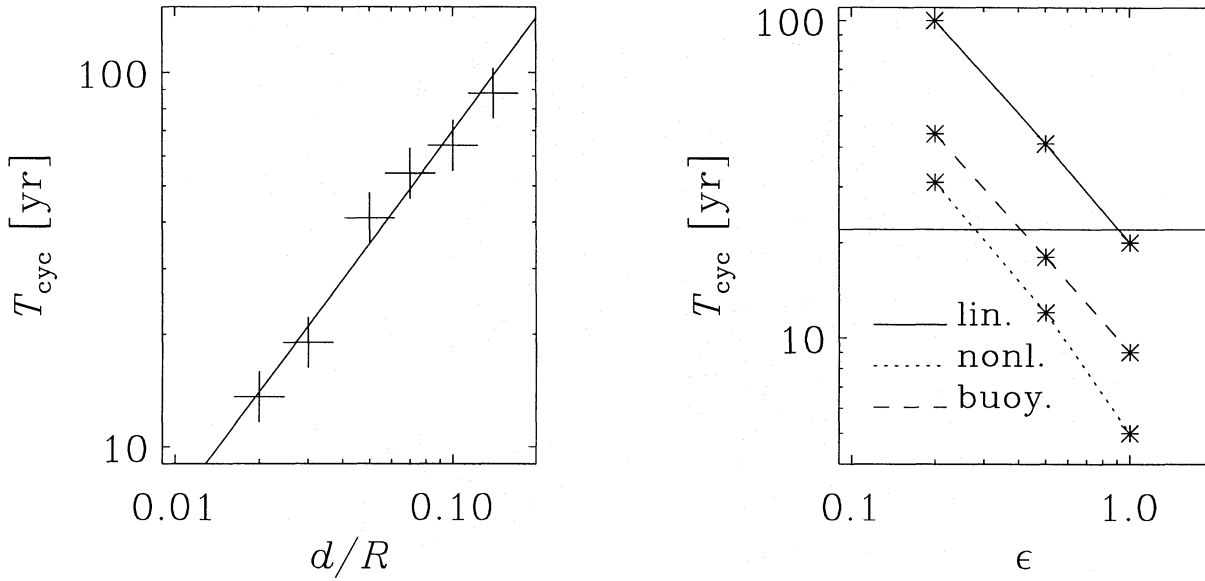


**Fig. 2.** Cycle period  $T_{\text{cyc}}$  as a function of  $d/R$  and  $\epsilon$  for  $\alpha_U = 0$ . In the left panel,  $\epsilon = 0.5$  is chosen and the results are well represented by the fit  $T_{\text{cyc}} = d [\text{yr}/\text{Mm}]$ . In the right panel,  $d/R = 0.05$  is used. The horizontal line indicates the solar cycle period of 22 yrs

**Table 1.** Summary of solutions for different values of  $\epsilon$ , for  $\alpha_U = 0$ ,  $T_{\text{rot}} = 25^{\text{d}}$ , and  $d/R = 0.05$

$\epsilon$	linear		nonlinear			nonl., buoy.		
	$c_\alpha$	$T_{\text{cyc}} [\text{yr}]$	$B_t^{\text{rms}} [\text{kG}]$	$B_p^{\text{rms}} [\text{G}]$	$T_{\text{cyc}} [\text{yr}]$	$B_t^{\text{rms}} [\text{kG}]$	$B_p^{\text{rms}} [\text{G}]$	$T_{\text{cyc}} [\text{yr}]$
1.0	0.031	20	1.8	2.8	5	3.3	13	9
0.5	0.015	41	3.3	3.4	12	5.3	11	18
0.2	0.006	100	6.0	2.9	30	8.4	7.1	44

zone proper and the radiative interior. Nonlocal mixing length theories predict that the thickness of the overshoot layer is  $d = 14 - 28 \text{ Mm}$  (Skaley & Stix 1991), and that the turbulent rms-velocity,  $u_t = \langle u'^2 \rangle^{1/2}$ , decreases from  $u_t^{(0)} \approx 20 \text{ m/s}$  to zero. We adopt a smooth profile for  $u_t$ :

$$u_t(r) = u_t^{(0)} \frac{1}{2} \left( 1 + \tanh \frac{r - r_0}{d} \right), \quad (21)$$

where  $r_0$  is the location of the bottom of the convection zone. We take  $r_0 = 0.7R$ , where  $R = 700 \text{ Mm}$  is the outer radius, and  $d$  is varied between  $0.02R$  and  $0.14R$ . For the correlation time we take  $\tau_{\text{corr}} = 10$  days, corresponding to the propagation time  $\ell/u_t$  with  $\ell = 20 \text{ Mm}$  and  $u_t = 20 \text{ m/s}$ . The Coriolis number is then  $\Omega^* = 5$ , which corresponds to the case of rapid rotation. Dynamos operating in the usual slow rotation limit with scalar  $\alpha$  and  $\eta_T$  are therefore not applicable to the overshoot layer.

Since  $\alpha$  is proportional to  $-d\eta_0/dr$ ,  $\alpha$  has a negative maximum at  $r = r_0$ , where the eddy diffusivity exhibits a strong gradient. This is in contrast to dynamos operating in the convection zone, where the  $\alpha$ -effect is governed by the negative density gradient rather than by the positive gradient of the turbulence intensity. In the convection zone the diffusivity is maximal. Below the overshoot region we adopt a reduced effective diffusivity that

is a hundred times smaller ( $\approx 3 \times 10^9 \text{ cm}^2/\text{s}$ ) than the value in the convection zone. In reality, this value should be a hundred times smaller still, but this is computationally more difficult, because then a larger range of different time scales would be involved in the problem.

The solar rotation law is considered as an input quantity and meridional flows are neglected. We adopt an inversion (Christensen-Dalsgaard & Schou 1988) of helioseismological data from the year 1988. We use a spline interpolation and assume rigid rotation at  $r = 0.5R$  (Fig. 1).

We solve the dynamo equation (1) using the code described by Brandenburg et al. (1992) for the profiles of  $\alpha$ ,  $\eta$ , and  $\Omega$  as specified above and extend the computational domain down to  $r = 0.5R$ . We restrict ourselves to purely dipole-type solutions by solving the equations in one hemisphere, using  $41 \times 41$  mesh points in the  $r$  and  $\theta$  directions. We determine both marginally excited (linear) solutions by adjusting  $c_\alpha$ , and  $\alpha$ -quenched (nonlinear) solutions with and without magnetic buoyancy. (In our models, the onset of dynamo action for magnetic fields of quadrupolar parity occurs at almost the same parameters as for dipolar parity.)

As characteristic output quantities we quote the magnetic cycle period ( $T_{\text{cyc}}$ ), as well as representative values for the poloidal

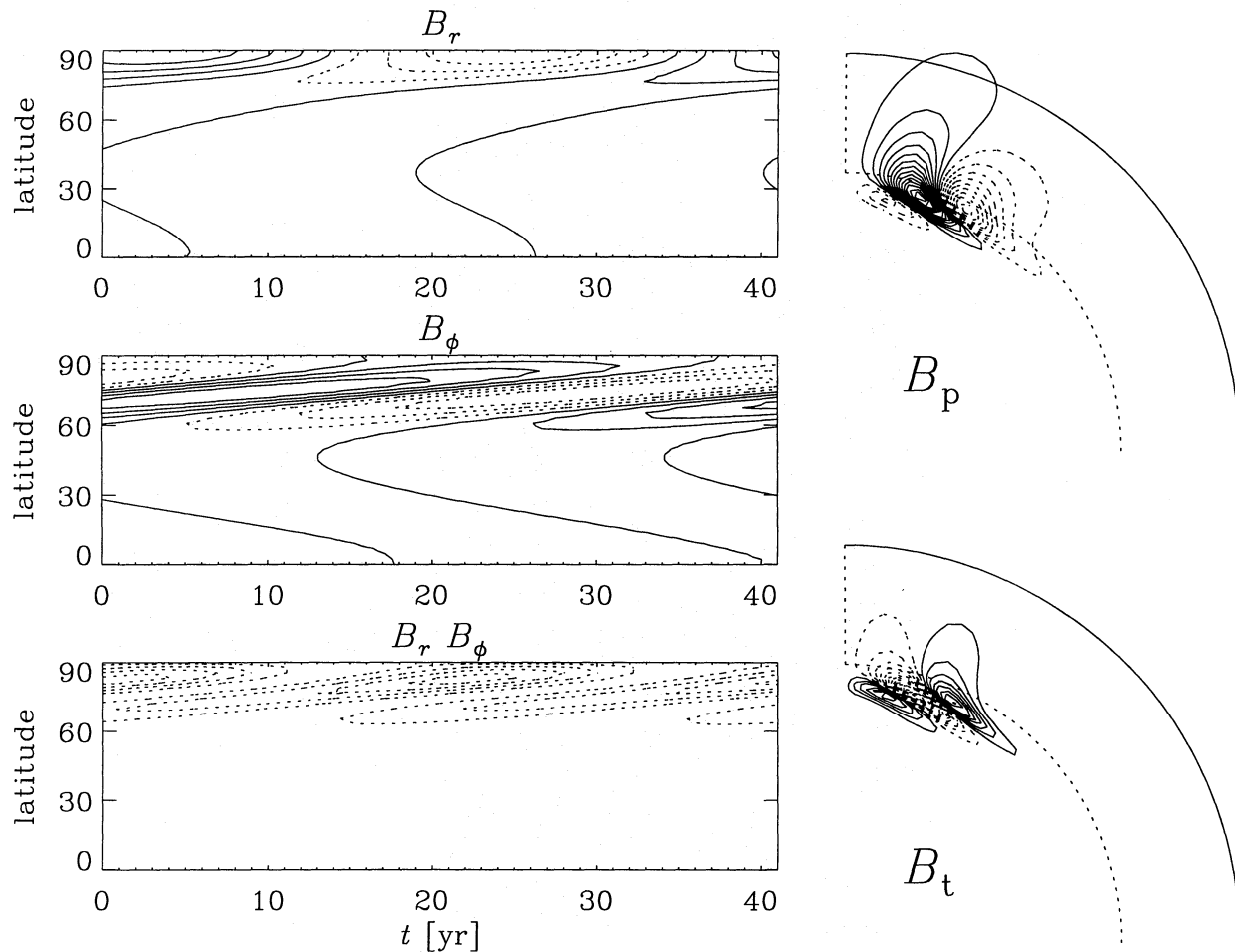


**Fig. 3.** The magnetic field geometry for the marginally excited solution with  $c_\alpha = 0.015$ ,  $\epsilon = 0.5$ ,  $d = 0.05R$ ,  $\alpha_U = 0$ . On the left, contours of  $\bar{B}_r$ ,  $\bar{B}_\phi$ , and  $\bar{B}_r \bar{B}_\phi$  are plotted as a function of time and latitude (butterfly diagrams).  $\bar{B}_r$  is taken at the surface, and  $\bar{B}_\phi$  the bottom of the convection zone. Dotted contours denote negative values. On the right, field lines of the poloidal field and contours of the toroidal field are drawn

and toroidal fields. We use a time average of the surface value of the poloidal root mean square field,

$$B_p^{\text{rms}} \equiv \left[ \int (\bar{B}_r^2 + \bar{B}_\theta^2) \sin \theta d\theta \Big/ \int \sin \theta d\theta \right]_{\text{surf}}^{1/2}, \quad (22)$$

and a time average of the toroidal root mean square field

$$B_t^{\text{rms}} \equiv \left[ \int \bar{B}_\phi^2 r^2 dr \sin \theta d\theta \Big/ \int r^2 dr \sin \theta d\theta \right]^{1/2}, \quad (23)$$

where the  $r$ -integral is taken from  $0.5R$  to  $R$ .

We also study the magnetic field geometry, plotting both cross-sections of the field in a meridional plane as well as contours of various fields as a function of time and latitude (butterfly diagrams). The butterfly diagram for the poloidal field is evaluated at the surface, while that for the toroidal field is taken at the bottom of the convection zone where the sunspot flux tubes are thought to be anchored. (The link between the toroidal field at the bottom of the convection zone and the location of sunspots could in principle be improved by invoking a model for the rise of magnetic flux tubes.)

#### 4. Cycle period and field strength

The cycle period may be considered as a main test of stellar dynamo theory, because it reflects an essential property of the dynamo mechanism. A realistic solar dynamo model should provide the correct 22 yr cycle period and, in the case of stellar cycles, the observed dependence of the cycle period on the rotation period.

In Table 1 we present models for different values of  $\epsilon$ . The dependence of the cycle period on  $\epsilon$  is shown in Fig. 2. For  $\epsilon \approx 1$  the linear solutions have the correct 22 yr solar cycle period. The cycle period increases approximately linearly with  $d$ :

$$T_{\text{cyc}} \propto d, \quad (24)$$

(see left panel of Fig. 2), which is in agreement with the linear relation for spherical shell dynamos (Roberts 1972). For very thin boundary layers the cycle time will thus become very short. Nonlinearity further shortens the cycle period and this effect has to be compensated for by taking a smaller value of  $\epsilon$  ( $\epsilon \approx 0.2 - 0.5$  depending on whether or not magnetic buoyancy is included).

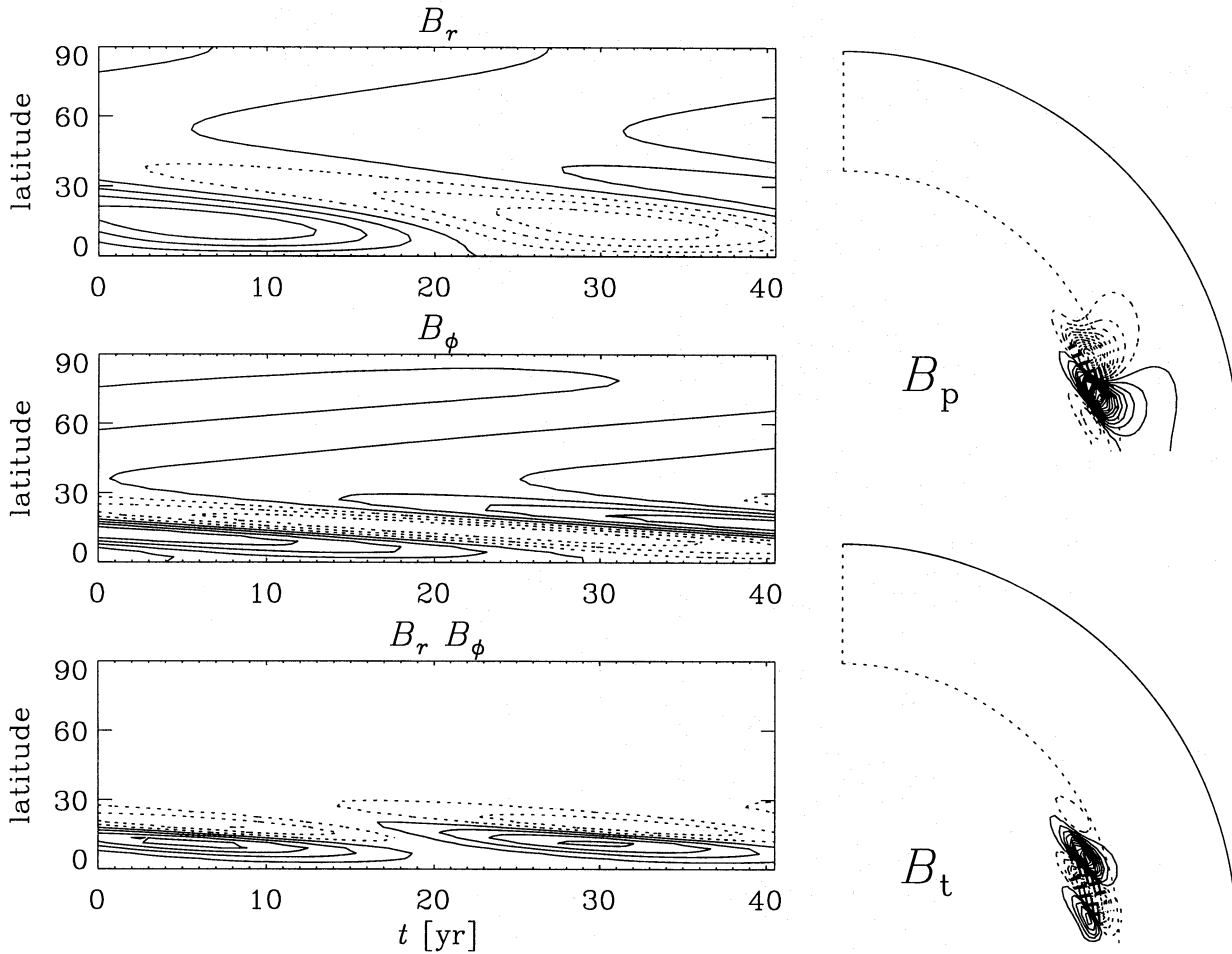


Fig. 4. The magnetic field geometry for the marginally excited solution with  $c_\alpha = 0.028$ ,  $\epsilon = 0.5$ ,  $d = 0.05R$ ,  $\alpha_U = 1$

In those cases where  $\alpha$ -quenching and magnetic buoyancy are included, the rms-values of the poloidal and toroidal fields are 11 G and 5 kG, respectively. Poloidal and toroidal fields as well as their mean and fluctuating parts are difficult to disentangle observationally. A toroidal field of 5 kG is, however, consistent with the observed total flux of  $10^{24}$  Mx, distributed over 50 Mm in depth and 400 Mm in latitude. On the other hand, a poloidal field of 11 G is maybe 5-10 times larger than the observed value.

In all cases the magnetic field exceeds the equipartition value. This is partly due to the turbulent diamagnetism leading to an accumulation of magnetic fields at the bottom of the convection zone, and partly due to too optimistic estimates for  $\alpha$ -quenching. It is possible that  $\alpha$ -quenching sets in for smaller field strengths (Tao et al. 1993), and this would reduce the values of  $B_p^{\text{rms}}$  and  $B_t^{\text{max}}$  by some factor. Also, inclusion of the macroscopic Lorentz force could lead to somewhat weaker magnetic field strengths (see Brandenburg et al. 1992). Its effect on the differential rotation profile, however, is expected to be small, because the observed cyclic variations of the solar angular velocity are only about 3 – 8%.

## 5. The butterfly diagram

For a thin overshoot layer ( $d = 0.02R$ ) there are too many field belts in each hemisphere. Better agreement with the solar field geometry is obtained for  $d = 0.05R$ . There is a pronounced “polar branch” of activity migrating from mid-latitudes to the poles, but at lower latitudes the toroidal field is too weak (Fig. 3). By choosing  $\alpha_U = 1$  (instead of  $\alpha_U = 0$ ) the field is enhanced at lower latitudes (Fig. 4), and the resulting butterfly diagram is now closer to the solar one.

At those latitudes where  $\partial\Omega/\partial r > 0$ , the poloidal and toroidal fields are in phase, which contradicts the observations. Such a rotation law will always produce positive  $\bar{B}_\phi$  from positive  $\bar{B}_r$  and *vice versa*. However, in the present models the field geometry is rather complicated and since the poloidal and toroidal fields are observed at different depths, a nontrivial phase relation may result. We therefore present in a third panel a butterfly diagram of  $\bar{B}_r \bar{B}_\phi$ . Note that at high latitudes the correct phase relation is recovered, because there  $\partial\Omega/\partial r$  is negative. However, close to the equator  $\bar{B}_r \bar{B}_\phi$  is usually positive. As expected, the overshoot dynamo does not provide a natural solution of the phase dilemma (cf. Schlichenmaier & Stix 1994).

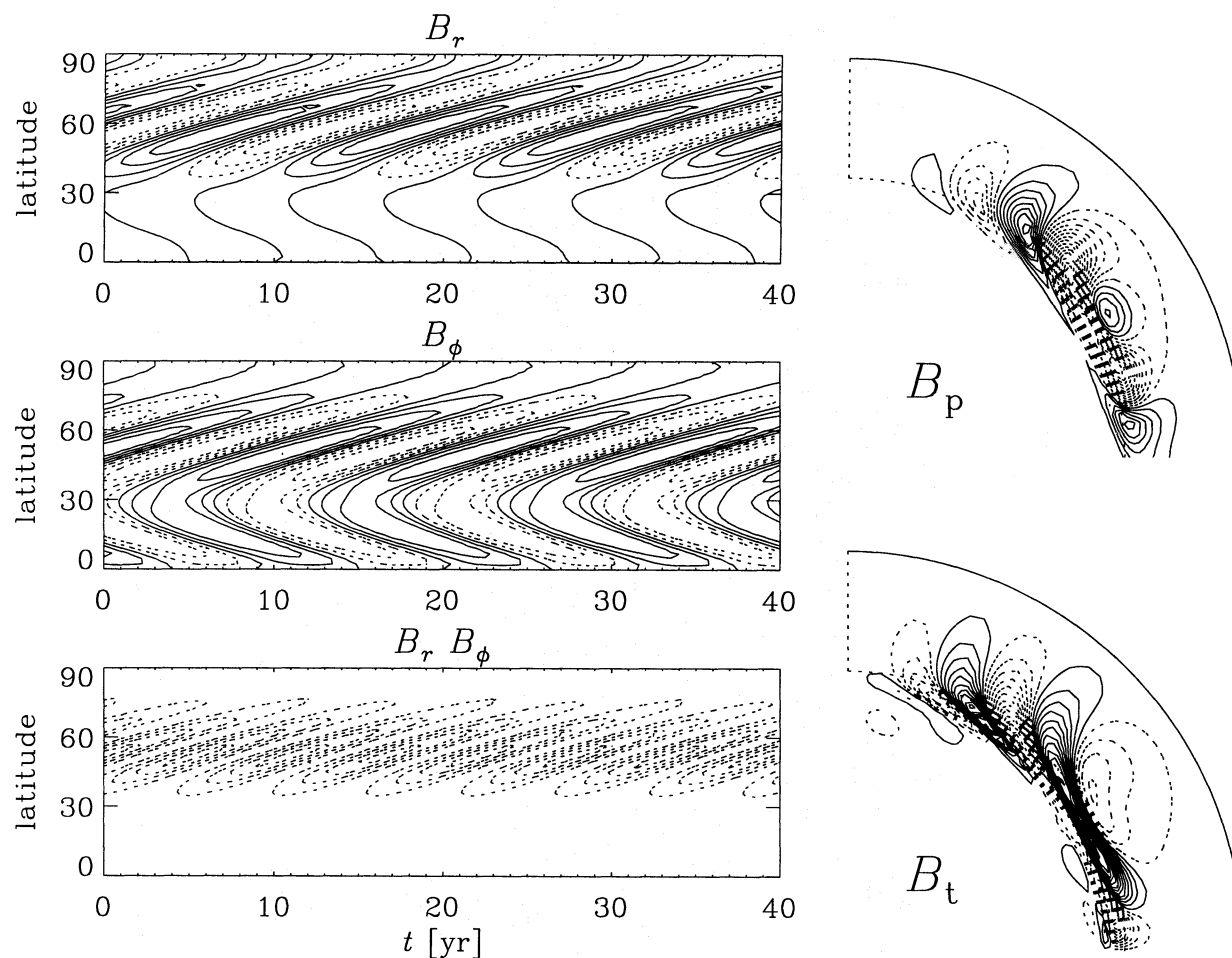


Fig. 5. The magnetic field geometry for the nonlinear ( $\alpha$ -quenched) solution without buoyancy and  $\epsilon = 0.5$ ,  $d = 0.05R$ ,  $\alpha_U = 1$

In Figs. 5 and 6 we display the field geometry for nonlinear models. The field is now more equally distributed over all latitudes. Note also that the field is strongly concentrated at the interface. The poloidal surface field is considerably weaker than the maximum toroidal field at the bottom of the convection zone (cf. Table 1).

## 6. Conclusions

We have explored the possibility of placing the solar dynamo in the overshoot layer using a realistic profile for the solar differential rotation and the full structure of the  $\alpha$  and  $\eta$  tensors for  $\Omega^* = 5$ , derived from a simple turbulence model. We have introduced two adjustable parameters  $\epsilon$  and  $\alpha_U$  that account for our ignorance of the intermittency of the magnetic field and the polar values of the  $\alpha$ -effect in stratified rotating turbulence. The effective thickness of the overshoot layer,  $d$ , is another parameter that is only known to within about 30% uncertainty. It is possible to adjust the dynamo parameters  $\epsilon$ ,  $\alpha_U$  and  $d$  such that the solar magnetic field geometry is reasonably well reproduced with a magnetic cycle period close to 22 years. The fact that the poloidal fields at the surface are too large by an order of mag-

nitude is probably related to incorrect quenching expressions whose form is unknown for rapid rotation.

The dilution factor  $\epsilon$  is the main free parameter that must be chosen such that the 22 years magnetic cycle period is obtained. The thickness of the overshoot layer must be chosen to match the correct number of toroidal field belts of the sun. Our results suggest that the thickness should not be much smaller than  $d = 0.05R \approx 35 \text{ Mm} \approx \frac{1}{2}H_p$ .

In deeper layers of the sun,  $\Omega^*$  exceeds unity, which leads to a number of new effects. For example, the magnetic field diffuses more efficiently along the rotation axis. This causes the poloidal field to emerge preferentially at high latitudes. This property is indeed seen in the sun where various indicators for the poloidal magnetic field geometry of the sun (e.g. polar faculae and the coronal green line) produce considerable activity at high latitudes in the form of the so-called polar branch. This appears to be similar to the emergence of flux tubes at high latitudes due to the influence of the Coriolis force (e.g. Schüssler & Solanki 1992).

Nonlinear effects typically lead to a reduction of the magnetic cycle period. Unfortunately, there are no consistent quenching expressions that are valid for rapid rotation. Mag-



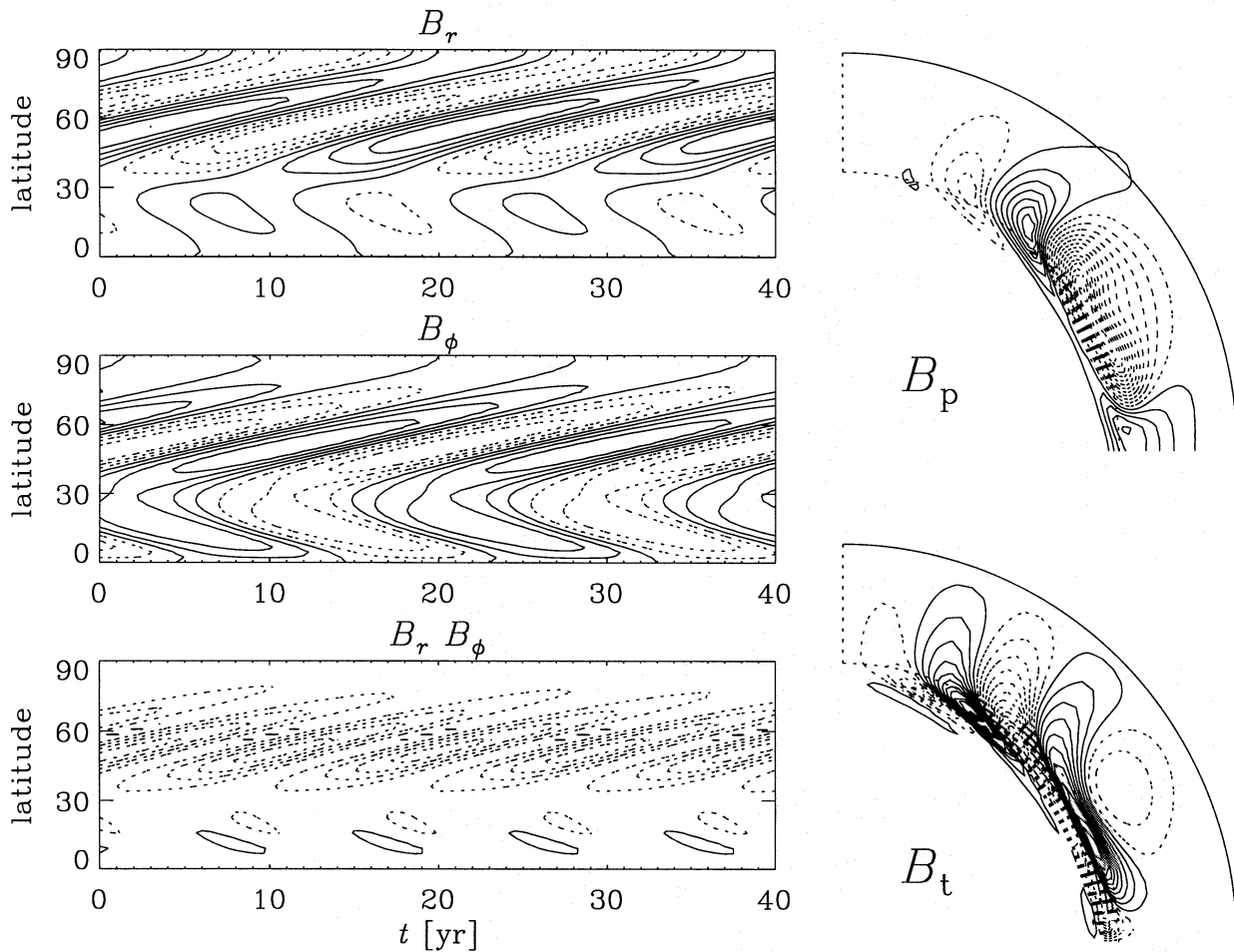


**Fig. 6.** The magnetic field geometry for the nonlinear ( $\alpha$ -quenched) solution with buoyancy and  $\epsilon = 0.5$ ,  $d = 0.05R$ ,  $\alpha_U = 1$

netic buoyancy also provides a nonlinear feedback (e.g. Durney & Robinson 1982; Moss et al. 1990), but recent computations by Kitchatinov & Pipin (1993) indicate that this leads to a mean field advection of a few m/s, which is well below the advection due to the diamagnetic effect. However, magnetic buoyancy is important in the upper layers (where the diamagnetic effect is weak), and can have significant effects on the field geometry and the cycle period. For models with magnetic buoyancy included (Fig. 6), the solar cycle period is obtained for  $\epsilon \approx 0.4$ . In the resulting butterfly diagrams for  $\bar{B}_r$  and  $\bar{B}_\phi$  typical features of the solar magnetic field geometry are reproduced, including the equatorward migration at low latitudes, and the polar branch at high latitudes. The polar branch, however, is still too strong in comparison to the equatorial branch. Apart from a narrow strip close to the equator, the sign of  $\bar{B}_r \bar{B}_\phi$  is negative, which is in agreement with the solar field. However, it remains to be investigated how meridional flows (omitted in the present paper) modify the field geometry. In any case, it remains rather unclear whether the results presented in Fig. 6 are solving the phase dilemma or not. The very clear out of phase relation of  $\bar{B}_r$  and  $\bar{B}_\phi$  stated in Stix (1976) is certainly not reflected by the given plots. Also, since both dipolar and quadrupolar fields

have similar excitation thresholds, it is not obvious why the solar field is almost perfectly dipolar. However, in the highly nonlinear regime the stability of solutions cannot be predicted based on the values of excitation threshold. We computed the solution presented in Fig. 6 for an initial condition with mixed parity such that the energies in the dipolar and quadrupolar parts were the same. We found that on a time scale of more than 1000 years the field approached the dipolar geometry studied in this paper.

Finally, we would like to recall that in order to model dynamo action in the overshoot layer, we have deleted terms in the expressions for  $\alpha$  that arise from the density stratification. This can be justified partially from three-dimensional simulations of cyclonic MHD convection, which do indeed produce a relatively small  $\alpha$  in the convection zone proper, but a much stronger (negative) peak in the overshoot layer. Formally, this can be reproduced by neglecting density stratification, even though the density is actually highly nonuniform.

*Acknowledgements.* We thank Paul Charbonneau and David Moss for suggesting improvements to the manuscript. W. Deinzer is acknowledged for his very careful refereeing of the submitted paper. A.B. was funded by the Advanced Study Program at NCAR.

## References

- Belvedere G., Proctor M.R.E., Lanzafame G., 1991, *Nature* 350, 481
- Brandenburg A., Moss D., Tuominen I., 1992, *A&A* 265, 328
- Brandenburg A., Krause F., Nordlund Å., Ruzmaikin A.A., Stein R.F., Tuominen I., 1993, *ApJ* (submitted)
- Carvalho J. C., 1992, *A&A* 261, 348
- Christensen-Dalsgaard J., Schou J., 1988, in: *Seismology of the Sun & Sun-like Stars*, (eds. V. Domingo, E.J. Rolfe), ESA SP-286, p. 149
- D'Silva S., 1993, *ApJS* 407, 385
- Durney B.R., Robinson R.D., 1982, *ApJ* 253, 290
- Durney B.R., De Young D.S., Passot, T.P., 1990, *ApJ* 362, 709
- Durney B.R., De Young D.S., Roxburgh I.W., 1993, *Solar Physics* 145, 207
- Ferrière K., 1993, *ApJ* 404, 162
- Gilman P.A., 1992, in: *The Solar Cycle*, (ed. K.L. Harvey), ASP Conference Series 27, p. 241
- Kaisig M., Rüdiger G., Yorke H., 1993, *A&A* 274, 757
- Kitchatinov L.L., Pipin V.V., 1993, *A&A* 274, 674
- Kitchatinov L.L., Rüdiger G., 1992, *A&A* 260, 494
- Kitchatinov L.L., Pipin V.V., Rüdiger G., 1994, *Astron. Nachr.* 315, 157
- Krause F., Rädler K.-H., 1980, *Mean-Field Magnetohydrodynamics and Dynamo Theory*, Akademie-Verlag Berlin
- Moreno-Insertis F., 1983, *A&A* 122, 241
- Moss D., Tuominen I., Brandenburg A., 1990, *A&A* 240, 142
- Nordlund Å., Brandenburg A., Jennings R.L., Rieutord M., Ruokolainen J., Stein R.F., Tuominen I., 1992, *ApJ* 392, 647
- Parker E.N., 1975, *ApJ* 198, 205
- Parker E.N., 1993, *ApJ* 408, 707
- Prautzsch T., 1993, in: *Theory of Solar and Planetary Dynamos*, (eds. P.C. Matthews, A.M. Rucklidge), NATO ASI, Cambridge University Press, p. 249
- Roberts P.H., 1972, *Phil. Trans. R. Soc. London, Ser. A* 272, 663
- Rüdiger G., Kitchatinov L.L., 1993, *A&A* 269, 581
- Schlichenmaier R., Stix M., 1994, in: *Solar Magnetic Fields*, (eds. M. Schüssler, W. Schmidt), Cambridge University Press, p. 107
- Schmitt D., 1987, *A&A* 174, 281
- Schmitt D., 1993, in: *The Cosmic Dynamo*, (eds. F. Krause, K.-H. Rädler, G. Rüdiger) IAU Symposium No. 157, Kluwer Acad. Publ., Dordrecht, p. 1
- Schüssler M., 1983, in: *Solar and stellar magnetic fields: Origins and coronal effects*, (ed. J.O. Stenflo), Reidel, Dordrecht, p. 213
- Schüssler M., 1987, in: *The internal solar angular velocity*, (eds. B.R. Durney, S. Sofia), Reidel, Dordrecht, p. 303
- Schüssler M., Solanki S., 1992, *A&A* 264, L13
- Skaley D., Stix M., 1991, *A&A* 241, 227
- Stix M., 1976, *A&A* 47, 243
- Tao L., Cattaneo F., Vainshtein S.I., 1993, in: *Theory of Solar and Planetary Dynamos*, (eds. P.C. Matthews, A.M. Rucklidge), NATO ASI, Cambridge University Press, p. 303
- Tuominen I., Rüdiger G., Brandenburg A., 1988, in: *Activity in Cool Star Envelopes*, (eds. Havnes et al.), Kluwer Acad. Publ., p. 13
- Vainshtein S.I., Zeldovich Ya.B., 1972, *Sov. Phys. Usp.* 15, 159
- Vainshtein S.I., Cattaneo F., 1992, *ApJ* 393, 165
- Yoshimura H., 1975, *ApJS* 29, 467
- Ziegler U., Yorke H.W., Kaisig M., 1994, *A&A* (submitted)

This article was processed by the author using Springer-Verlag L<sup>A</sup>T<sub>E</sub>X A&A style file version 3.